Xinguang Cheng
Sagnik Basuray
Satyajyoti Senapati
Hsueh-Chia Chang

Department of Chemical and Biomolecular Engineering, Center for Microfluidics and Medical Diagnostics, University of Notre Dame, Notre Dame, IN, USA

Received March 9, 2009
Revised May 24, 2009
Accepted May 26, 2009

Research Article

Identification and separation of DNA-hybridized nanocolloids by Taylor cone harmonics

A rapid (minutes) electrospray bead-based DNA hybridization detection technique is developed by spraying a mixture of hybridized and unhybridized silica nanocolloids. With proper far-field control by external electrodes, the trajectory of the ejected nanobeads from the electrospray is governed by specific harmonics of the Laplace equation, which select discrete polar angles along well-separated field maxima near the conducting Taylor cone. Due to Rayleigh fission and evaporation, beads of different size acquire different total charge after ejection and suffer different normal electrophoretic displacement such that they are ejected along well-separated field maxima and are deposited in distinct rings on an intersecting plane. As the hybridized DNA is of the same dimension as that of the nanocolloid, the nanocolloids are hence easily differentiated from the unhybridized ones. This technique is highly specific as the high shear stress in the microjet shears away any non-specifically bound DNA from the nanocolloid surface.

Keywords:
DNA / Electrospray / Harmonics / Hybridization / Nanocolloids
DOI 10.1002/elps.200900159

1 Introduction

Electrospray has been extensively used as an ionization source for MS [1], differential mobility analyzers [2], synthesis of biodegradable microfiber [3], microencapsulation [4] and nanotechnology [5]. The use of electric field in electrospray atomizes the liquid drops from the Taylor cone, which continually disintegrate into several droplets of smaller radius due to evaporation and Rayleigh fission until only analyte is left with the charges [6, 7]. There is increasing effort to utilize this phenomenon to differentiate the electrophoretic mobility of charged bioparticles like bacteria and other solid bioaerosols [8]. The bioparticles having different size and intrinsic surface charges could be separated after ejection. With their larger size and Peclet number compared with molecules, bioparticles' charging and ejection from a Taylor cone are insensitive to thermal noise and hence permits techniques like differential mobility analysis to be performed at atmospheric conditions. Bioparticle analysis would hence require less elaborate and more portable equipment than molecular MS.

Correspondence: Professor Hsueh-Chia Chang, Department of Chemical and Biomolecular Engineering, University of Notre Dame, 182 Fitzpatrick Hall, Notre Dame, IN 46556, USA
E-mail: hchang@nd.edu
Fax: +1-574-631-8366

Abbreviations: EDC, 1-ethyl-3-(3-dimethylaminopropyl) carbodiimine hydrochloride**; NHS,** sulfo-*N*-hydroxysulfosuccinimide

Moreover, as will be demonstrated for the first time in this article, with proper far-field control, the particle electrophoretic trajectories exhibit intriguing patterns of lines or bands with clear separation, which could be used as a fingerprint line or band spectrum for bioparticles such as vesicles and endosomes with a distribution of mass and surface charge. For nanocolloids with small dimension (~100 nm), we shall show that each line/band will be shown to favor particles of certain size range, with the natural nanocolloid surface charge playing an insignificant role. As a result, the line patterns allow us to decipher the size distribution of the particles and, in the case of a binary suspension of nanocolloids, the relative amount of each.

Mobility analysis is a powerful method in the nucleic acid-based diagnostics that has evolved rapidly in the past decades [9]. Nucleic acid-based diagnostics offer the capability to identify most microbes such as bacteria and viruses and contribute immensely to epidemic control, environmental monitoring and anti-terrorism/biowarfare applications. The development of modern diagnostic technique is driven by reduced detection time and cost, portability, higher sensitivity and specificity [10, 11]. Nanocolloids, with the large surface-to-volume ratio and the short diffusion time they offer, have become a surface assay technique of choice. Recently, Senapati *et al.* demonstrated a rapid, portable and inexpensive genetic detection bead-based microfluidic platform for field application [12]. Taton *et al.* report that the sensitivity of the nanoparticle-based method is about two orders of magnitude higher than that of the corresponding fluorophore-based DNA-array scheme [13]. Gagnon *et al.* used silica nanoparticles and present a

dielectrophoretic hybridization detection and analysis scheme [14]. They found that the dielectrophoretic mobility of the beads is sensitive to DNA hybridization reactions in the target ssDNA solution below nanomolar concentrations.

In this article, we report a rapid electrospray bead-based DNA hybridization detection platform by electrospraying a mixture of hybridized and unhybridized silica nanocolloids obtained by hybridizing fluorescently labeled target ssDNA with complementary oligo probe functionalized silica nanobeads. In a recent paper [15], we reported that nanoparticles of difference sizes are segregated upon electrospraying and are deposited as discrete lines on the substrate. As the hybridized DNA is expected to significantly increase the nanoparticle size, the same technique can be used to detect hybridization. It hence combines the sensitivity and rapid hybridization advantages of nanocolloid surface assay with the fast separation/identification features of particles mobility analyzers. The distinct line patterns we have found allow extremely discriminating separation and identification sensitivity. This technique is very rapid and takes only 5 min to differentiate between hybridized and unhybridized beads. The size of the hybridized beads increases substantially from the unhybridized one due to the stretching of long target ssDNA under the high electric field. The increase in size of beads due to hybridization facilitates the separation from beads without any molecular target. This electrospray bead-based detection platform is highly specific due to the high shear stress of the ejected liquid that shears away nonspecifically bound DNAs on the beads surface.

2 Materials and methods

The electrospray bead-based detection platform mainly comprises five steps: (i) experimental setup and working solution, (ii) functionalization of oligomer probe on beads, (iii) asymmetric PCR amplification, (iv) bead-based hybridization of target species and (v) colloid spectrometry by electrospray. *Escherichia coli* and green crab DNA are used as test samples to study the detection of hybridization by this electrospray bead-based platform. Each step is described briefly in the following section.

2.1 Experimental setup and working solution

Conventional spray experimental setup is designed to generate the Taylor cone and is schematically represented in Fig. 1. High direct current voltage is generated using A HCZE-30PNO25-LD high voltage power supply (Matsusada Precision Device, Tokyo). A steel microneedle (Hamilton, 91033) with nominal outer diameter 210 μm and thickness 50 μm is filled with the working solution and mounted on a glass stage 1 mm in height. The counter electrode pair consists of two parallel strips of copper tape with a gap of 2.5 mm and are placed about 2.0 mm away from the needle tip. This allows sufficient separation gap between the Taylor cone and the ground

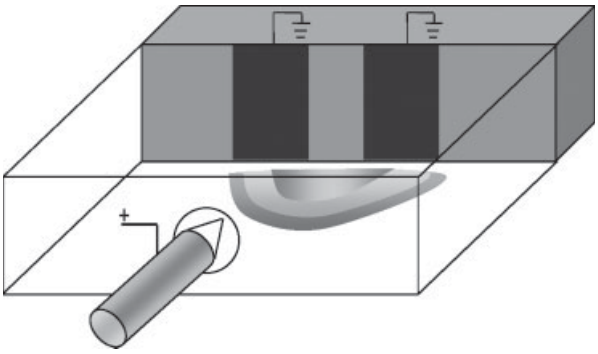

Figure 1. The experimental setup for electrospray with symmetrically placed ground electrodes.

electrode to obtain a clear colloidal pattern independent of the evaporating liquid. Individual nanocolloid depositions are imaged with an inverted fluorescent microscope (Olympus IX-71) and are recorded by a high performance quantitative digital CCD camera (QImaging Retiga-EXL).

A mixture of 80% DI water and 20% ethanol is used as a working solution to avoid the precipitation of DNA in higher concentration of ethanol. The conductivity is carefully adjusted to 200 μs/cm by the addition of sodium chloride. The use of ethanol is necessary to create low surface tension of the working solution so that a stable Taylor cone can be generated under direct current field.

A suspension of nanocolloids consisting of fluorescently labeled polystyrene particles of three different sizes (980, 400 and 250 nm) is used to generate a control pattern and calibration standard depending on different particle size. The fluorescently labeled polystyrene nanocolloids are purchased from Polyscience.

2.2 Functionalization of oligomer probe on beads

To facilitate DNA hybridization, the carboxylated silica beads (Corpuscular) are functionalized with target specific 27-mer oligo probes (Invitrogen), complimentary to the target species DNA. It is achieved by coupling with water-soluble carbodiamide (EDC) and sulfo-*N*-hydroxysulfosuccinimide (NHS). This results in a linkage between the oligo and carboxy groups by an amide bond. More specifically, the silica beads are thoroughly washed three times with MES (pH 5.5) activation buffer. The beads are then stirred with a mixture of EDC and NHS for 30 min. Initially, EDC reacts with carboxyl group present on the bead surface forming an *o*-acyl ester intermediate. This intermediate is very unstable and in the absence of any amine group, it reacts with water (due to electron deficient carbon center) regenerating the carboxyl group. Thus, another coupling reagent NHS is added to form semi-stable intermediate, which is highly reactive toward amine [16]. This amine reactive ester intermediate subsequently reacts with an amine functionalized oligo probe in 1× PBS buffer to construct DNA attached to silica bead by amide linkages.

2.3 Asymmetric PCR amplification

To avoid recombination of dsDNA before hybridization, asymmetric PCR is performed to produce ssDNA. Asymmetric PCR is similar to normal PCR except that an unequal molar concentration of primers is used to amplify ssDNA. Initially, the amplification starts exponentially, but as the lower concentrated primer is exhausted, the higher concentrated primer continues to amplify only one strand of DNA, thus producing ssDNA. The final ssDNA product is the complimentary of excess primer used in amplification. An asymmetric PCR reaction is performed using a fluorescently labeled forward PCR primer in excess to amplify ~1000 bp *E. coli* ssDNA to study DNA detection. The concentration of amplified ssDNA is around 100 nM.

2.4 Bead-based hybridization of target species

The hybridization of oligo functionalized silica beads and target ssDNA is carried out in 4× saline-sodium citrate buffer after careful washing of the functionalized beads. The target ssDNA and functionalized silica beads are hybridized by constant stirring at a precisely controlled temperature of 50°C for 6 h. After hybridization, the beads are washed in 1× PBS to remove any non-specific attachment of ssDNA from silica bead surface. Finally, all the beads are mixed in 0.1 nM working solution to perform electrospray for detection of DNA hybridization.

3 Results and discussion

3.1 Discrete deposition patterns of nanocolloids

We demonstrate the size-sensitive selection of discrete trajectories by depositing a ternary nanocolloid suspension with increasing particle sizes of 250, 400 and 980 nm on the substrate between the Taylor cone and ground electrodes. Different fluorescent excitation differentiates the different nanocolloids, which produce a rainbow-like pattern away from the cone as shown in Fig. 2. The 980 nm particles deposit into a half circle furthest from the cone with a polar angle of about 42.5°. The 400 nm and 250 nm particles select two separated half rings with polar angles of about 58.7 and 78.4°, and the 250 nm particles land closer to the cone. These half circles are segments of the concentric bands around the Taylor cone axis.

The deposition pattern is contrary to what is expected for a parabolic free fall due to gravity – the nanocolloids with the largest size travel the furthest and are deposited in the inner most half circles. For particles below 1 μ, the electrophoretic force is estimated to be six orders of magnitude higher than gravitational force. The primary mechanism for the concentric rainbow is due to the harmonics of the conducting Taylor cone [15]. The Taylor cone free-surface electrostatics selects certain discrete harmonics of the Laplace equation defined by the

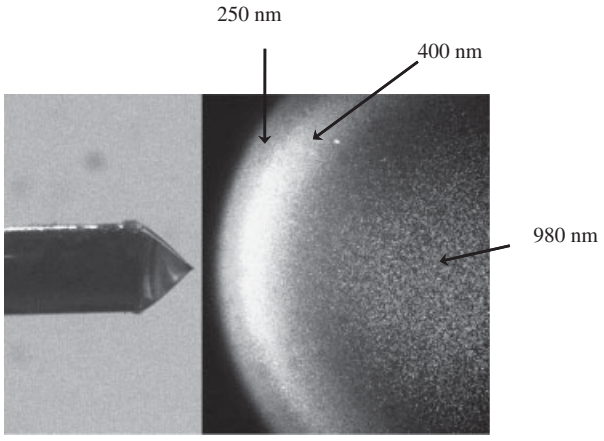

Figure 2. The ternary pattern with different modes selected by the 980, 400 and 250 nm nanocolloids.

usual Legendre polynomial in spherical coordinates, $\phi_n = r^n P_n(\cos\theta)$[6], such that $r^n P_n(\cos\theta_0) = 0$ for a conducting cone. The cone angle of $\theta_0 = 49^\circ$ is determined by $n = 0.5$ to produce a Maxwell pressure that also scales as r^{-1} as the singular azimuthal capillary pressure of the cone. An additional number of discrete axisymmetric spherical harmonics can actually be selected by the conducting Taylor cone with the above angle θ_0 for non-integer mode numbers $n = 0.5$, 1.89234, 3.27519, 4.65525, 6.03413, 7.41242, 8.79037, *etc.* (see Table 1). The field intensity of the modes decays with mode number, with only the $n = 0.5$ mode providing a singular field to sustain a singular Maxwell force to compensate the singular capillary force. Between 0 and 90° from the cone axis, the most two dominant modes ($n = 3.27519$ and 4.65525) exhibit three field maxima off the cone axis with cone angles 42.8, 58.7 and 78.4°. (The field maximum of $n = 1.89234$ is not within this first quadrant.) As such, the sprayed nanoparticles can select these three dominant field maxima and eject in discrete specified trajectories. In the ternary pattern of Fig. 2, the 980 nm particles select angle 42.80°, while 400 and 250 nm particles select angle 58.7 and 78.4°. Similar separations of liquid droplets of different sizes have been observed [17, 18] but the connection to the harmonics is observed for the first time in [15] and here.

Which field extrema the colloids select depend on their transverse distribution near the jet tip at the outer periphery of the cone, which is controlled by their local transverse electrophoretic displacement in the spray region roughly corresponding to the region where the isopotential lines nest together in Fig. 3, before the different harmonics are separated by more than a nanocolloid dimension. In this spray region, the electric force is not imparted on the nanocolloid directly but on a larger liquid drop that encapsulates it. The ejection of this drop distorts the cone tip [18] and imparts a transverse electrophoretic force on the ejected drop radially away from the axis. The transverse displacement in this spray region depends on the residence time of the drop in the region and hence its axial velocity u_z, which is directly related to the net charge of the drop.

Table 1. The nanocolloids size spectrum in Taylor cone harmonics

Diameter of particle (nm)	Angle (°)	Harmonics mode *n*
100	82.3	8.79037
250[a)]	78.4	4.65525
400[b)]	58.7	3.27519
980	42.7	4.65525

a) Both functionalized silica nanobeads and polystyrene nanobeads.

b) Both *E. coli*-hybridized silica nanobeads polystyrene nanobeads.

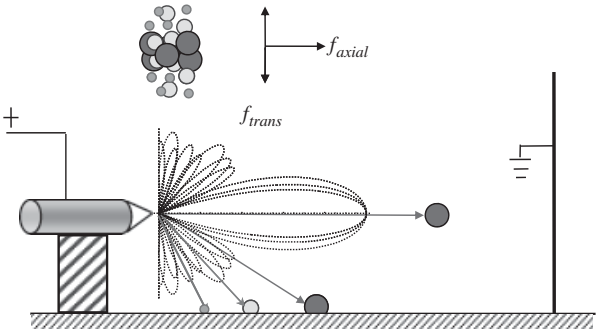

Figure 3. Equipotential lines of the axisymmetric harmonics of a conducting Taylor cone in spherical coordinates whose origin lies at the cone tip. Rays along the field maxima of the different harmonics produce rings.

The observed deposition patterns thus suggest that the larger particles have a higher net charge and electrophoretic velocity and are hence deflected less from the cone axis, while the smaller ones suffer from larger displacement. The charged solution on any particle is believed to lose liquid by charge-retaining evaporation and Rayleigh fission due to Coulombic repulsion [18]. For a liquid drop, this liquid/charge loss continues until the radius reaches the Rayleigh radius R governed by $q = 8\pi(\varepsilon_0 \gamma R^3)^{1/2}$ [19]. Liquid and charge loss from the nanocolloids is expected to proceed until this equilibrium drop radius R is identical to the particle radius a and the charge is left on the particle. Due to the electrospray running in positive mode, the net charge on the particles become positive, even though the surface charge of the polystyrene particle is negative in the aqueous solution. As such, the axial velocity scales as $u_z \sim a^{1/2}$, which is strongly dependent on the particle size. Therefore, the selection of the discrete harmonics is entirely governed by colloid size, with very little contribution from the surface charge on the nanocolloid. Smaller colloids have a smaller net charge, a smaller axial velocity, a larger residence time in the spray region (larger flight time) and hence a larger transverse displacement. They hence occupy harmonics with larger angle in the far field (Fig. 3), as is consistent with the deposition pattern in Fig. 2. To verify that particles of the same size deposit at the same position regardless of their surface charge, we have sprayed 250 nm silica beads and latex particles and found them to land at the same position (see Table 1).

As a final verification of our omission of gravitational and inertial forces, we estimate from the above mechanism that the residue charge on a 250 nm nanocolloid to be 5.75×10^{-16} C and, with field strength of about 1×10^4 V/cm in our experiment, we estimate the electrophoretic force to be about 0.575 nN. The corresponding gravitational force is 2.17×10^{-16} N. The terminal velocity due to the electrophoretic force is estimated to be 5.73 m/s and is reached within 0.2 μs. Since the flight time is roughly 0.4 ms, inertial effect is unimportant for the deposition of nanocolloids by this mechanism.

3.2 Detection of DNA

We first test single strand *E. coli* DNA, ~1000 bp or 300 nm fully stretched, on the electrospray-based platform. Two hundred and fifty nanometer nanoparticles are chosen, to have a sufficient size difference between the hybridized nanobeads and unhybridized beads. The result after running the electrospray experiment for about 5 min is shown in Fig. 4A. The position of the hybridized nanobeads is identified by its fluorescent signal, activated by ~466 nm wavelength and captured on camera. In brightfield, we can see the unhybridized beads that land closer to the cone though they are spread over a larger area due to the diffusion and cover the hybridized beads region also.

Hybridized beads select the angle of about 58.7°, where the electric field of the harmonics mode $n = 3.27519$ reach a maximum. This angle is the same as that selected by the 400-nm beads. It is interesting to note that the 250-nm functionalized beads (without the DNA) occupy the same angle of 78.4° as the 250-nm unfunctionalized nanobeads. As such, the diameter of the hybridized beads is around 400 nm, indicating a near doubling of the size of the nanobeads. Electrokinetic stretching of DNA has been investigated in liquid solutions, such as λDNA, which is found to be stretched in liquid solutions under an electric field of the order of 25 V/cm [20]. The applied field in our electrospray experiment is 1×10^4 V/cm. Thus we speculate that the near doubling of the bead size is because the hybridized DNAs are fully stretched on the nanobead.

We have also successfully detected green crab DNA, ~500 bp or about 150 nm fully stretched. We choose the 100 nm beads to match the DNA size. The detection result as shown in Fig. 4B shows a similar pattern as the *E. coli* DNA. The hybridized beads deposit in a specified band by selecting an angle of about 78.4°, which is the same angle as occupied by 250-nm beads. This gives, thus, a direct proof of DNA stretching, as the stretched green crab DNA on the bead surface gives a resultant hybridized bead size of 250 nm. The unhybridized nanocolloids select a higher angle of 82.3°, where the electric field of the harmonic mode $n = 8.79037$ exhibits a field maximum. We tabulate the

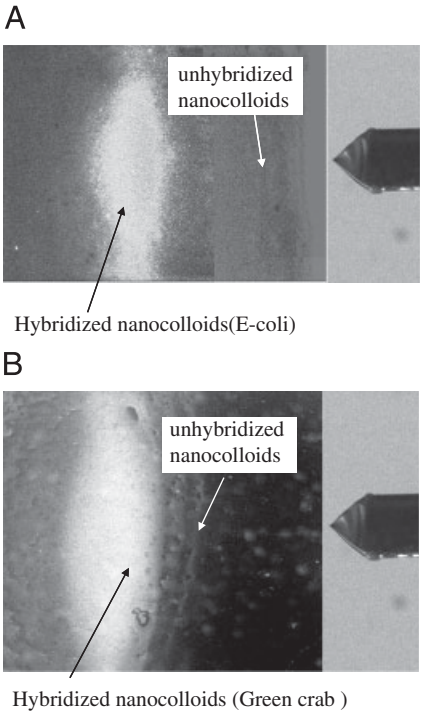

Figure 4. The separation and identification of DNA-hybridized nanocolloids. (A) Green crab DNA hybridized on nanobeads of 100 nm and (B) *E. coli* DNA hybridized on nanobeads of 250 nm.

results in Table 1 to include all nanocolloids sizes, angle and the corresponding Taylor cone harmonics mode.

The non-target DNA can also bind to the functionized beads during hybridization. However, we found that the large shear stresses because of high flow near the Taylor cone tip can remove the non-target DNA. The beads accumulate at the cone tip first and then eject out with the liquid. At a flow rate of about 1.0 μL/min, the velocity at the tip is $U = 1.0$ m/s for a microjet diameter of 1 μm. This results in a shear force on the DNA of length $L = 100$ nm to be $f_s = \mu UL \sim 0.1$ nN. As the DNA binds to the bead by hydrogen bond with the oligoprobes on the surface, with hydrogen bond having a typical energy of about 20 kJ/mol with the characteristic length of about 2 Å in water, the binding force is also about 0.1 nN, which is of the same order as the shear force. As such, shear stresses at the Taylor cone tip is high enough to shear away non-specifically bound target DNA, without a sufficient number of hydrogen bonds, thus providing high specificity for genetic identification.

4 Concluding remarks

To conclude, we present here a rapid and inexpensive DNA detection platform using the novel concept that the harmonics of the Taylor cone and the electrophoretic force on each nanocolloid is sensitive to its size. Due to their small dimension, the hybridization of single strand target DNAs onto nanocolloids can significantly increase the size, particularly if the DNA is fully stretched because of the applied voltage. Thus the hybridized nanocolloids select a harmonic field extremum and deposit along a single line or a band that is well separated from the deposition location of the unhybridized nanocolloids. Our preliminary results suggest that the relative position and the angle of the hybridized band and the unhybridized one can give a quantitative estimate of the DNA size. The concentration of the DNA can also be estimated by labeling the DNAs with fluorophores and using a microscope to estimate the fluorescent intensity of each line. Alternatively, microelectrode arrays can be fabricated at the deposition location to measure the current carried by the charge-carrying nanocolloids to estimate the number of nanocolloids deposited on each line – and precisely determine the line location. The shear-enhanced specificity is yet another advantage of this technique. This generic method can be extended to detect RNA/biomarker docking on oligomer probe, biomarker probe or any other types of probes functionalized on nanocolloids. Finally, we have focused on hybridization detection in this report. With the rapid detection our method offers, the bottleneck now resides at the hybridization step and a rapid hybridization technique must be developed before this new detection method can become competitive against other slower detection methods without hybridization.

The authors would like to thank Nishant Chetwani and Dr. Başar Bilgiçer for their valuable inputs. This work is financially supported by DTRA (HDTRA1-08-C-0016) and Great Lake Protection Fund.

The authors have declared no conflict of interest.

5 References

[1] Fenn, J. B., Mann, M., Meng, C. K., Wong, S. F., Whitehouse, C. M., *Science* 1989, *246*, 64–71.

[2] de la Mora, J. F., de Juan, L., Eichler, T., Rosell, J., *Trends Anal. Chem.* 1998, *17*, 328–339.

[3] Yeo, L. Y., Gagnon, Z., Chang, H.-C., *Biomaterials* 2005, *26*, 6122–6218.

[4] Loscertales, G., Barrero, A., Guerrero, I., Cortijo, R., Márquez, M., Gañán-Calvo, A. M., *Science* 2002, *295*, 1695–1698.

[5] Salata, O. V., *Curr. Nanosci.* 2005, *1*, 25–33.

[6] Taylor, G. I., *Proc. R. Soc. London. Ser. A* 1964, *280*, 383–397.

[7] Rayleigh, L., *The Theory of Sound*, Dover, New York 1945.

[8] Flagan, R. C., *Electrical Techniques in Aerosol Measurement*, Wiley, New York 2001.

[9] Mothershed, E. A., Whitney, A. M., *Clin. Chim. Acta* 2006, *363*, 206–220.

[10] Barken, K. B., Haagensen, J. A. J., Tolker-Nielsen, T., *Clin. Chim. Acta* 2007, *384*, 1–11.

[11] Chang, H.-C., *AICHE* 2007, *53*, 2486–2494.

[12] Senapati, S., Mahon, A. R., Gordon, J., Novak, C., Sengupta, S., Powell, T. H. Q., Feder, J. *et al.*, *Biomicrofluidics* 2009, *3*, 022407.

[13] Taton, T. A., Mirkin, C. A., Letsinger, R. L., *Science* 2000, *289*, 1757–1760.

[14] Gagnon, Z., Senapati, S., Gordon, J., Chang, H.-C., *Electrophoresis* 2008, *29*, 4808–4812.

[15] Cheng, X., Chang, H.-C., *New J. Phys.* 2009 (in press).

[16] Marquette, C. A., Blum, L. J., *Top. Curr. Chem.* 2006, *261*, 113–129.

[17] Tang, K., Gomez, A., *Phys. Fluids* 1994, *6*, 2317–2332.

[18] Barrero, A., Loscertales, I., Marquez, M., *Mater. Res. Soc. Symp. Proc.* 2005, *860E*, LL5.9.1–LL5.9.6.

[19] Lebarle, P., Tang, L., *Anal. Chem.* 1993, *65*, 972–986.

[20] Ferree, S., Blanch, H. W., *Biophys. J.* 2003, *85*, 2539–2546.

